Journal Pre-proof

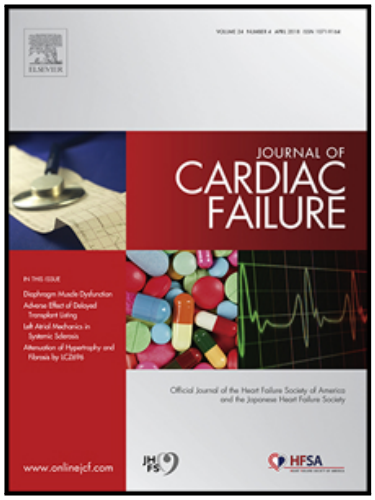

Cardiac thyrotropin-releasing hormone (TRH) inhibition improves ventricular function and reduces hypertrophy and fibrosis after myocardial infarction in rats.

Mariano L. Schuman PhD , Ludmila S. Peres Diaz PhD , Maia Aisicovich BSc , Fernando Ingallina MD , Jorge E. Toblli MD, PhD , Maria S. Landa PhD , Silvia I. García PhD

PII: S1071-9164(21)00124-X
DOI: https://doi.org/10.1016/j.cardfail.2021.04.003
Reference: YJCAF 4751

To appear in: *Journal of Cardiac Failure*

Received date: 23 October 2020
Revised date: 11 March 2021
Accepted date: 6 April 2021

Please cite this article as: Mariano L. Schuman PhD , Ludmila S. Peres Diaz PhD , Maia Aisicovich BSc , Fernando Ingallina MD , Jorge E. Toblli MD, PhD , Maria S. Landa PhD , Silvia I. García PhD , Cardiac thyrotropin-releasing hormone (TRH) inhibition improves ventricular function and reduces hypertrophy and fibrosis after myocardial infarction in rats., *Journal of Cardiac Failure* (2021), doi: https://doi.org/10.1016/j.cardfail.2021.04.003

Highlights

- Cardiac TRH inhibition after myocardial infarction reduces fibrosis and hypertrophy
- TRH silencing after myocardial infarction upregulates HIF-1α mRNA and its protein
- Cardiac TRH inhibition strategy improves ventricular function after infarction

Cardiac thyrotropin-releasing hormone (TRH) inhibition improves ventricular function and reduces hypertrophy and fibrosis after myocardial infarction in rats.

Mariano L. Schuman PhD [1,2], Ludmila S. Peres Diaz PhD *[1,2], Maia Aisicovich BSc *[1,2], Fernando Ingallina MD [1,5], Jorge E. Toblli MD, PhD [4], Maria S. Landa PhD [1,2,3], Silvia I. García PhD [1,2,4].

[1] University of Buenos Aires, School of Medicine, Institute of Medical Research A. Lanari, Ciudad Autónoma de Buenos Aires, Argentina.

[2] National Scientific and Technical Research Council (CONICET), University of Buenos Aires (UBA), Institute of Medical Research (IDIM), Department of Molecular Cardiology, Ciudad Autónoma de Buenos Aires, Argentina.

[3] National Scientific and Technical Research Council (CONICET), University of Buenos Aires (UBA), Institute of Medical Research (IDIM), Department of Molecular Genetics and Biology of Complex Diseases, Ciudad Autonoma de Buenos Aires, Argentina.

[4] Laboratory of Experimental Medicine, Hospital Alemán, Ciudad Autonoma de Buenos Aires, Argentina.

[5] University of Buenos Aires (UBA), School of Medicine , Institute of Medical Research "Alfredo Lanari," Department of Cardiology, Ciudad Autonoma de Buenos Aires, Argentina.

*These authors contributed equally to this work.

Short Title: TRH inhibition improves ventricular function

Correspondence

Silvia Inés García, PhD. Molecular Cardiology Laboratory Head, Institute of Medical Research (UBA-CONICET), Combatientes de Malvinas 3150, CP: 1427, Ciudad Autónoma de Buenos Aires, Argentina.Phone number: +54-11-5287-3904

Email:garcia.silvia@lanari.uba.ar; garcia.silvia@conicet.gov.ar; marianoschuman@conicet.gov.ar

Abbreviations

LV left ventricle, LVH left ventricular hypertrophy, SHR spontaneously hypertensive rat MI myocardial infarction, PCR polymerase chain reaction, siRNA small interference RNA *ANP*, Atrial *natriuretic* peptide. *BNP*, B-type natriuretic peptide *βMHC*, beta *myosin heavy chain* TGFβ, Transforming growth factor -β1 VEGF, *Vascular endothelial growth factor* IVSd, Interventricular Septum thickness in diastole; IVSs, Interventricular Septum thickness in systole; LVIDd, left ventricular internal diameter in diastole; LVIDs, left ventricular internal diameter in systole; LVPWd, Left ventricular posterior wall thickness in diastole; LVPWs, Left ventricular posterior wall thickness in systole; LVEDV, Left ventricular end diastolic volume; LVESV, Left ventricular end systolic volume; SF, shortening fraction; EF, Ejection fraction; SV, Stroke volume; HR, Heart rate.

Abstract

Background

Cardiac thyrotropin-releasing hormone (TRH) is a tripeptide with still unknown functions. We demonstrated that the left ventricle (LV) TRH system is hyperactivated in spontaneously hypertensive rats and its inhibition prevented cardiac hypertrophy and fibrosis. Therefore, we evaluated whether *in vivo* cardiac TRH inhibition could improve myocardial function and attenuate ventricular remodeling in a rat model of myocardial infarction (MI).

Methods and Results

In Wistar rats, MI was induced by a permanent left anterior descending coronary artery ligation. A coronary injection of a specific siRNA against TRH was simultaneously applied. The control group received a scrambled siRNA. Cardiac remodeling variables were evaluated one week later. In MI rats, TRH inhibition decreased LV end-diastolic (1.049±0.102 vs. 1.339±0.102 ml, $p<0.05$), and end-systolic volumes (0.282±0.043 vs. 0.515±0.037 ml, $p<0.001$), and increased LV ejection fraction (71.89±2.80 vs. 65.69±2.85 %, $p<0.05$). Although both MI groups presented similar infarct size, siRNA-the TRH treatment attenuated the cardiac hypertrophy index and myocardial interstitial collagen deposition in the peri-infarct myocardium. These effects were accompanied by attenuation in the rise of TGFβ, collagen I, and III and also the fetal genes (ANP, BNP, and βMHC) expression in the peri-infarct region. Besides, the expression of Hif1α and VEGF significantly increased compared to all groups.

Conclusions

Cardiac TRH inhibition improves LV systolic function and attenuates ventricular remodeling after MI. These novel findings support the idea that TRH inhibition may serve as a new therapeutic strategy against the progression of heart failure.

KEYWORDS:

thyrotropin-releasing hormone; myocardial infarction, fibrosis, cardiac hypertrophy, small interference RNA

Introduction:

Thyrotropin-releasing hormone (TRH) is a small neuropeptide (p-Glu-His-Pro-NH2) initially identified in the hypothalamus. The TRH gene (*Trh* in rodents) encodes a TRH precursor with several copies of the tripeptide, the number of which depends on the species.

TRH is widely distributed in the central nervous system(24) and other extraneural tissues(8). TRH also has effects on the cardiovascular system of rodents, because its intracerebroventricular or intravenous administration increases blood pressure, heart rate, and contractility(23). The hypertensive effect of TRH seems to be independent of the thyroid system(11, 19, 25).

Previous studies have demonstrated that the TRH system is present in the rat heart(5, 35), and induces cardiac contractility in isolated rat hearts (32).

Also it was described that the left ventricle (LV) TRH system is hyperactivated in the hypertrophied left ventricle (LV) of adult spontaneously hypertensive rats (SHR). Indeed, cardiac TRH inhibition prevents cardiac hypertrophy despite the fact that severe hypertension still develops. These findings suggest that TRH is involved in the hypertrophy process of the SHR(29). Moreover, we observed that the intracardiac overexpression of TRH induced by the injection of a specific plasmid (PCMV-TRH) in the LV of a normal Wistar rat leads to a hypertrophic heart phenotype characterized by the increase of hypertrophic markers expression (ANP, BNP and β-MHC)(30). Furthermore, Jin et al.(17) identified *Trh* as one of the genes induced in the LV of rats with heart failure, up to 8 weeks after myocardial infarction. They also suggested that TRH may have a long-term detrimental effect in rats with ischemic cardiomyopathy(17).

Based on these results, it was postulated that TRH plays an autocrine or paracrine role in cardiac physiology.

Although both TRH mRNA and protein were found in human heart tissue(4, 15, 28), the role of endogenous TRH in ischemic myocardium and myocardial remodeling after infarction remains unknown.

In this study, we developed a long term specific inhibition of the LV TRH system to evaluate the participation of TRH in post-ischemic remodeling. We hypothesize that its inhibition could attenuate tissue damage and improve ventricular function after myocardial infarction.

In addition, Hypoxia-inducible factor 1 (Hif-1α) a well-known regulator of the hypoxic response after myocardial infarction, is up-regulated in regions of myocardial infarction and ischemia (21), and protects against the extension of infarction and improves border zone survival (18). As HIF-1α is known to induce transcription of several genes, including VEGF (31) and regulate the oxidative stress of heart tissue (31), we studied both pathways and postulated that Hif-1α may be regulated by TRH.

Altogether, our results indicate a novel and cardioprotective role of the inhibition of the cardiac TRH system in the non-reperfused myocardium.

Methods:

Ethics statement.

All experiments were performed in accordance with the "*Guide for the Care and Use of Laboratory Animals*" (US National Institutes of Health Publication No. 85-23, National Academy Press, Washington, DC, revised 1996) .The protocol was approved by the Institutional Animal Care and Use Committee CICUAL UE-IDIM (IDIM-CONICET, Buenos Aires, Argentina) Number: 019-14. All protocols were performed under anesthesia, and all efforts were made to minimize suffering.

All reagents were from Sigma (St. Louis, MO) unless otherwise indicated.

Animals.

16 week-old male Wistar rats (12 rats/group, Charles River Laboratories) were housed in a room with controlled temperature (23 +/- 1°C) under a 12:12-h light-dark schedule.

Model of Myocardial Infarction (MI) and siRNA injection

The animals were divided in four groups of 12 animals each as follows: Sham+siRNA-Control, Sham+siRNA-TRH, Infarct+siRNA-Control and Infarct+siRNA-TRH. At the end, animals from each group were used for anatomopathology (n=6/per group) and biochemical and molecular (n=6/per group) studies.

Male Wistar rats (16 weeks old; 350 to 450 g) were anesthetized with an intraperitoneal injection of ketamine (90 mg/kg) and xylazine (10 mg/kg), intubated and ventilated (Harvard Apparatus respirator, model 683; South Natick, Massachusetts).

After a left thoracotomy, MI was produced by permanent ligation of the left anterior descending coronary artery (LAD) about 3–4 mm from the top of the left atria using 6-0 prolene suture. The suture was not tied in control rats (sham group).

The rats were randomized into different treatment groups after LAD ligation. Within one minute after coronary ligation, 40 µg of siRNA against TRH or siRNA scrambled in 200 µL of saline was injected using an insulin syringe directly into the anterior wall of the left

ventricle after ligation of the LAD. This dose was chosen based on our prior studies (29). Intramyocardial injections were performed in multiple sites of the LV free wall (apex to base), by slowly injecting the solution while withdrawing the syringe. The siRNA gene transfer to the normal hearts was performed with the same technique without ligation of the LAD. After the procedure, the chests were closed with a continuous 6–0 prolene suture, followed by a suture to close the skin and the rats were allowed to recover. After surgery, all rats received antibiotics (10 mg ampicillin intramuscularly) and analgesia tramadol clorhidrate 5mg/kg intraperitoneally for 24hr.

Specific stealth™ iRNAs from Invitrogen (CA, USA) were used as previously described(29), which present a chemical modification resulting in lower toxicity and higher stability. This modification eliminates concerns about sense strand off-target effects as previously described (27).

For the iRNA selection, the Block-iT™ iRNA Designer software was used. A mix of two double-strand sequences against *Trh* (TRH-iRNA498 and TRH-iRNA138) and a mix of two control iRNA sequences carrying mismatches compared with the specific ones (Con-iRNA498 and Con-iRNA138) were used, and whose sequences are as follows:

TRH-iRNA498: S: 5´ACGGUCCUGGUUACCAGAUUUCUUU3´ and
AS: 5´AAAGAAA UCUGGUAACCAGGACCGU3´;

TRH-iRNA138: S: 5`GAUCUUCACCCUAACUGGUAUCCCU3´ and
AS: 5`AGGGAUACCAGUUAGGGUGAAGAUC3`;

Con-iRNA498: S: 5´ACGCCGUUGAUCCGAUAUUCUGUUU3´ and
AS: 5´AAACAGAAUAUCGGAUCAACGGCGU3´;

Con-iRNA138: S: 5´GAUCACUAUCCGUCAUAUGCUCCCU3´ and
AS: 5´AGGGAGCAUAUGACGGAUAGUGAUC3´

The screening of known rat genes from genomic databases of the National Center for Biological Information using the Blast program indicates specificity of the sequence

used in the iRNA design and confirms their 100% homology with the rat preproTRH gene (*Trh*).

Echocardiography

6 days after the MI surgery we performed Transthoracic Echocardiography with the Ultramark 9 Ultrasound system using a 10-MHz linear transducer on anesthetized animals.

The two-dimensional parasternal short-axis imaging plane was used to obtain M-mode tracings at the level of the papillary muscles. Left ventricular (LV) internal dimensions and LV wall thickness were determined at systole and diastole using leading-edge methods and guidelines of the American Society of Echocardiography (10).

Left ventricular end-diastolic diameter was measured at the time of the maximal left ventricular end-diastolic diameter. In contrast, left ventricular end-systolic diameter was assessed at the time of the most anterior systolic excursion of the posterior wall.

Ejection fraction was also calculated and used as an ejective index of systolic function.

The measurements included: Interventricular septum diastolic and systolic dimension (IVS Thickness d, s), Left ventricular posterior wall thickness (systolic and diastolic) (LVPW Thickness s, d), Left ventricle end-diastolic and systolic volume (LVEDV, LVESV), Stroke volume (SV), Ejection fraction and fractional shortening (EF, FS). All measurements were based on the average of three consecutive cardiac cycles and were performed by one observer who did not know the previous results.

Histology, Infarct size and Image Analysis

For histologic analysis, Hearts were perfused with saline solution through the abdominal aorta until they were free of blood. Hearts were frozen and sectioned transversely from

apex to base into 2-mm slices and then immediately sliced with a scalpel into 1-mm-thick sections perpendicular to the long axis of the heart. These slices were used to measure the infarct size by TTC. For fibrosis measurement, the tissues was fixed in 10% buffered formalin solution (pH 7.2) and were embedded in paraffin, and 5-um-thick sections were cut from the midsection of the heart, at the level of the papillary muscles. The fibrosis was measured from LV circumference in Masson's trichrome and Sirius red-stained sections with a digital image analysis system. Three pictures were taken from each heart for later analysis.

Infarct size.

Hearts were frozen and sectioned transversely from apex to base into 2-mm slices. To delineate the infarct size, tissue sections were incubated in 1% (wt/vol) triphenyltetrazolium chloride (TTC) (Sigma) in PBS (pH 7.4) at 37C for 15 min allowing differentiation between the viable (red) and necrotic areas (pale) of the myocardium. For each section, the infarct size was measured from enlarged digital photos. MI percentage was calculated as the infarcted area divided by the area of the whole LV of the section. Cumulative areas for all tissue sections from each heart were used for the comparisons. All tissue samples were evaluated independently by two investigators without prior knowledge of the group to which the rats belonged. All measurements were carried out using an image analyzer (Image-Pro Plus version 4.5 for Windows, Media Cybernetics, LP, Silver Spring, Maryland, USA).

Using sections stained with Sirius red (SR), and Masson's Trichrome-stained 5-µm paraffin-embedded sections visualized by polarized light microscopy, the infarction scar was measured as a percentage from the LV circumference. Fibrosis was measured by the Nikon program E400 light microscope (Nikon Instrument Group, Melville, N.Y., USA), from five representative fields from the infarcted myocardium region. Collagen

areas in infarcted and noninfarcted regions were determined (X40 magnification) using brightfield illumination.

To verify the efficiency of the *Trh* gene inhibition by siRNA, tissue sections were stained with an anti–TRH precursor specific antibody as previously described (26).

Immunohistochemical evaluation

Immunolabelling was carried out, as previously described(26), using a modified avidin-biotin-peroxidase technique (Vectastain ABC kit, Universal Elite; Vector Laboratories, California, USA). Following deparaffinization and rehydration, sections were washed in PBS for 5 min. Quenching of endogenous peroxidase activity was achieved by incubating the sections for 30 min in 1% hydrogen peroxide in methanol. After washing in PBS (pH 7.2) for 20 min, the sections were incubated with blocking serum for a further 20 min. After that, the sections were rinsed in PBS and incubated with a biotinylated universal antibody for 30 min. After a final wash in PBS, the sections were incubated for 40 min with Vectastain Elite ABC reagent (Vector Laboratories, California, USA) and exposed for 5 min to 0.1% diaminobenzidine (Polyscience, Warrington, Pennsylvania, USA) and 0.2% hydrogen peroxide in 50 mmol/L Tris buffer (pH 8). For the purpose of evaluating TRH precursor content by immunohistochemistry, the specific anti-rat TRH precursor polyclonal antibody was used at a dilution of 1:300 (sc-366754, Santa Cruz, Inc., USA), for TGF-β1 a polyclonal antibody was used at a dilution of 1:400 (ab92486, Abcam Cambridge, MA) and for collagen type I a rabbit polyclonal antibody was used at a dilution 1:50 (ab90395, Abcam, Cambridge, MA). For the evaluation of collagen type III content (167-5M, Biogenex, CA, USA mouse monoclonal antibody was used at a dilution 1:40 and for HIF1α (A4.951) NB100-131, Novus Biologicals, LLC, USA) mouse monoclonal antibody was used at a dilution 1:700. For

VEGF was used at a dilution 1:500 (sc-7269, Santa Cruz Biotechnology, Dallas, TX, USA), For Thioredoxin was used at a dilution 1:200 (ab86255, from Abcam, Cambridge, UK), for Peroxiredoxin was used at a dilution 1:300 (ab15571, from Abcam, Cambridge, UK), for Nitrotyrosine was used at a dilution 1:300 (#MAB5404; Millipore, Burlington MA, USA), for HSP70 was used at a dilution 1:200 (sc-1060, from Santa Cruz Biotechnology, Dallas, TX, USA) and anti-HSP27 was used at a dilution 1:200 (sc-1048 from Santa Cruz Biotechnology, Dallas, TX, USA). (Images 600x). Three pictures were taken from each heart for later analysis. Sections across the experiments were stained at the same time and conditions for all the groups.

Quantitative real-time RT-PCR.

Quantification of *Trh*, *collagen type III (Col3a1)*, *collagen type I (Col1a1), BNP (Nppb), βMHC (Myh7), ANP (Nppa), TGFβ (Tgfb1), VEGF (Vegfa), GLUT4 (Slc2a4), Caspase 3 (Casp3), GATA4 (Gata4)* and *HIF1α (Hif1a)* mRNA expression was performed using a real-time RT-PCR technique normalized by *beta actin (Actb)* housekeeping gene expression. Briefly, for cDNA synthesis,

2 µg of total RNA and 1 µg of random hexamer primers (Promega) were heated followed by incubation at 4°C. After RT reaction (Promega), real-time PCR was performed using a Bio-Rad iQ iCycler Detection System (Bio-Rad Laboratories) with SYBR green fluorophore. Reactions (in duplicate) were carried out in a total volume of 20 µl. A three-step protocol (95°C for 30 s; 60, 64, or 66°C annealing for 30 s; and 72°C extension for 40 s) was repeated for 43 cycles. Rat primers (Invitrogen) for rat *Trh*, rat *BNP (Nppb),*, rat *collagen type III (Col3a1)*, and rat *beta actin (Actb)* were as previously described (29).

Additional primers were designed as follows:

TGFβ1: Forward 5'-CAATGGGATCAGTCCCAAAC-3' and reverse 5'-GTTGGTATCCAGGGCTCTCC-3',

ANP: Forward 5'-GATGGATTTCAAGAACCTGCT-3' and reverse 5'-CGCTTCATCGGTCTGCTC-3',

βMHC: Forward 5'-ATCCTCATCACCGGAGAATC3' and reverse 5'-GGTTGGCTTGGATGATTTGA-3',

Collagen type I A1 : Forward 5'-GATGATGGGGAAGCTGGTAA-3' and reverse 5'-CCTCTGTGTCCCTTCATTCC-3',

VEGF: Forward 5'-GCCCATGAAGTGGTGAAGTT-3' and reverse 5'-ACTCCAGGGCTTCATCATTG-3',

GLUT4: Forward 5'-TGCCCGAAAGAGTCTAAAGC-3' and reverse 5'-TGGACGCTCTCTTTCCAACT-3',

caspase3: Forward 5'-CAAGTCGATGGACTCTGGAA-3' and reverse 5'-TGACATTCCAGTGCTTTTATGG-3',

GATA4: Forward 5'-CCCCAATCTCGATATGTTTGA-3' and Reverse 5'-GCCGGTTGATACCATTCATC-3',

HIF1α: Forward 5'-CGATGACACGGAAACTGAAG-3' and reverse 5'-TTCGAAGTGGCTTTGGAGTT-3'

Melt curve analysis was performed after every run to ensure a single amplified product for every reaction. The authenticity of the amplicons generated was confirmed by their size on a 2% agarose gel. It was also used as reference genes *GAPDH (Gapdh)*, *HPRT (Hprt1),* and *beta-actin (Actb)* was chosen.

No differences were found between any of the experimental groups in the *beta-actin (Actb)* housekeeping gene by the GeNorm software. Quantification was done by

normalizing the (cycle threshold) Ct values of genes of interest with respect to beta-actin Ct ones by applying the $2^{-\Delta\Delta}$CT method.

Biochemical and pathology experiments.

After one week, rats were weighed, and tibia long index was measured before rats were killed by decapitation. Blood samples were collected, and thyroid hormone levels were measured from serum using a chemiluminescent enzyme immunometric assay (EICLIA) (Roche, Buenos Aires, Argentina). Hearts were rapidly removed and weighed. The non-infarcted region of the LV (counterpart of the infarcted area, remote zone) from each rat was cut and stored until analysis. In some animals, cardiac tissues (atria, LV, right ventricle, and septum) were separated for the quantification of mRNA expression (n=6); others without separating cardiac tissues were used for pathology experiments (n=6).

Cell culture and simulated ischemia

We used the model described by Bès S et al(3) with modifications. H9c2 embryonic rat heart-derived (ventricular) cells (myoblasts) from ATCC (American Type Culture Collection, Manassas, VA, USA) were cultured in Dulbecco's modified Eagle's medium (DMEM)/F12, with 4,5 g/L glucose supplemented with 10% fetal bovine serum (FBS) and 1% gentamicin/streptomycin (v/v) with trans retinoic acid (10nM) under 95% air/ 5% CO2, and subcultured when at 50–60% confluence.

One day before transfection, cells were plated in a 6 well plate in growth medium without antibiotics with 10nM trans Retinoic acid. Transfections were performed at 60%70% confluence using Lipofectamine 2000 as described previously(26, 30). Cells

were incubated in Opti-MEM I Reduced Serum Medium (Invitrogen) with or without RNAi–Lipofectamine 2000 complexes (50 nM) (2 μg/ml) for 16 h and then replaced with fresh DMEM with FBS or hypoxic medium with trans retinoic acid and antibiotics.

Hypoxia consisted of layering mineral oil (2ml) over a thin film of the hypoxic medium that covered the cells for 2 hours before culturing the cells in serum-deficient DMEM for 24hours. Then, cells were harvested for mRNA extraction. The hypoxic medium (prebubbled with N_2 gas) was an HEPES-buffered medium containing (in mmol/L) 139 NaCl, 4.7 KCl, 0.5 MgCl2 , 0.9 CaCl2 , 5 HEPES, pH 7.4. The control plates were kept in normoxic conditions with 300ul of mineral oil (not layering) and were cultured in parallel for each condition of the same time as the experimental groups.

Statistics.

Values are expressed as means ± standard deviation (SD) except where indicated. All statistical analyses were performed using absolute values and processed using Statistics (version 6.0, Software). The assumption test to determine Gaussian distribution was performed by the Kolmogorov-Smirnov method. For parameters with Gaussian distribution, comparisons between groups were carried out using one-way ANOVA followed by Bonferroni's test, Kruskal-Wallis test (nonparametric ANOVA), and Dunn's multiple comparison test when appropriate. In the case of two groups, mean comparisons were performed using a *t*-test or Mann-Whitney test when necessary. *P* values of <0.05 were considered significant

Results:

siRNA-TRH inhibition effect on survival rate and infarct size

siRNA-TRH or siRNA-Control was injected into the infarct and border zone immediately after coronary ligation.

There were no differences in the survival rates of MI siRNA-TRH compared to MI siRNA-Control treated animals 1week follow-up -MI (74% vs. 70%, respectively).

Additionally, there was no difference in infarct size between the MI siRNA-Control and MI siRNA-TRH groups, measured by triphenyltetrazolium (TTC) method (32 ± 3.3 % and 30 ± 3.1 % respectively).

Effects of MI on *TRH* expression

We found a significant increase in the expression of myocardial *TRH* precursor mRNA ($p<0.001$) in the peri-infarct area of infarcted rats respect to sham when injected with siRNA-Control. The increase in *TRH* precursor mRNA abundance was significantly reduced by four-fold with the siRNA-TRH treatment (Figure 1A). In agreement, LV immunohistochemistry showed an enhanced positive brown signal corresponding to TRH precursor peptide levels in the peri-infarct area of the MI siRNA-Control group, which was significantly attenuated ($p<0.01$) in the peri-infarct area of the MI siRNA-TRH group. These results confirmed that MI increases TRH expression at both gene and protein levels, and these changes were effectively blocked by the specific siRNA-TRH treatment. It is worthy to note that there was low basal expression of TRH in sham hearts (Figure 1B).

Furthermore, cardiac siRNA treatment against *TRH* did not alter plasma thyroid hormone levels in any group indicating that the results were independent of the thyroid system (Supplemental Figure1). There were also no significant TRH mRNA expression differences in pancreas or hypothalamus in any group (data not shown).

siRNA-TRH inhibition reduces hypertrophy in response to MI

The hypertrophy index expressed as heart weight to body weight ratio (HW/BW) was significantly higher in MI group compared to non-infarcted controls both treated with siRNA-Control, indicating the presence of MI-induced hypertrophy. Conversely, infarcted rats treated with siRNA-TRH showed a HW/BW similar to that of sham controls, and then significantly lower than siRNA-Control-treated infarcted rats (Figure 2A). There were no significant differences between body weights in the MI groups (data not shown).

Consistent with hypertrophy index, echocardiography performed six days after LAD ligation showed a markedly increase in interventricular septum (IVS) thickness and left ventricular internal (LVI) diameter, corresponding to postinfarction hypertrophy. The Inhibition of TRH in the MI group significantly lowered diastolic IVS thickness and LVI diameter (systolic and diastolic) compared with the control group (Table 1).

Additionally, to confirm the effects of siRNA-TRH inhibition on cardiac remodeling, we examined the expression of several genes associated with hypertrophy in areas around the infarct border zone. Consistent with the macroscopic results, there was a significant more than 2-fold increase in the mRNA expression of *ANP (Nppa*), *BNP* (*Nppb*)*,* and *β-MHC* (*Myh7*) in the MI siRNA control rats respect to the sham group. When TRH was silenced, these MI-associated gene expressions were significantly decreased compared to those observed in MI siRNA-Controls (Figure 2B).

All these data indicate that siRNA-TRH inhibition prevented cardiac hypertrophy in the peri-infarct region induced by MI.

siRNA-TRH inhibition improves cardiac function following MI

As shown in Table 1, six days after LAD ligation the Infarcted siRNA-Control group, presented a markedly decrease in shortening fraction (SF) and ejection fraction (EF)

with an increase in the left ventricular cavity areas at diastole and systole (LVEDV and LVESV, respectively) respect to sham. These changes are pathognomonic of the postinfarction myocardial failure. The inhibition of TRH, significantly lowered LVEDV, LVESV, and increased EF compared to the infarct siRNA-Control group. Shortening fraction tended to rise in MI siRNA-TRH treated animals, although this observation was not statistically significant. Heart rate significantly increased in the infarcted group with siRNA-Control compared to sham, whereas it was significantly lower in the siRNA-TRH, reaching levels similar to those observed in sham animals.

Sham-operated animals did not present myocardial dysfunction as assessed by echocardiography.

Altogether these results confirm a protective effect and an improvement on the cardiac function mediated by LV TRH inhibition in the infarcted rats.

siRNA-TRH inhibition reduces myocardial fibrosis following MI

Based on the TRH-induced profibrotic effects previously observed in SHRs(29) and to further investigate whether the siRNA-TRH delivery influenced the morphology of the heart, we analyzed the fibrotic status. Interstitial fibrosis in the peri-infarct area of the LV infarcted rats significantly increased by more than 15 fold compared to sham rats as shown by Sirius red and Masson's technique. The collagen deposition in the MI siRNA-TRH treated group was significantly reduced compared to MI siRNA-Control group (p<0.01) (Figures 3A and 3B). No difference was observed in the collagen deposition of the scar between the groups.

Additionally, we measured the expression of fibrosis marker genes *TGFβ*, *Collagen* type I, and type III. As expected, there was a significant more than two-fold increase in their expression in the peri-infarct area of the infarcted control rats compared to the sham. As

hypothesized, their expressions were significantly diminished in the MI siRNA-TRH group respect to MI control group (Figures 4 A, B, C).

To reinforce these findings, we performed heart immunohistochemistry (Figures 4 D, E, F). In MI siRNA-Control rats, the protein expression of TGFβ, Collagen I and Collagen III significantly increased (p<0.01) compared to the sham rats. In contrast, silencing TRH in the MI groups significantly reduced the protein immmunostaining of TGFβ, Collagen I and Collagen III in the peri-infarct area compared to MI siRNA-Control. siRNA-TRH treatment did not affect cardiac collagen deposition in sham rats.

Collectively, these data demonstrated that, siRNA-TRH inhibition not only improves LV function but also ameliorates the morphology of infarcted hearts after MI by reducing the fibrosis in the infarct border zone.

siRNA-TRH inhibition increase Hif1α and VEGF following MI

To further investigate the molecular mechanisms underlying the effect of TRH inhibition on the ischemic heart, we measured the mRNA expression of *HIF1α*. We observed a significant increase in *HIF1α* mRNA abundance in the MI siRNA-TRH treated group compared to MI siRNA-Control and sham-treated groups (Figure 5A). There was no evident increase in *HIF1α* mRNA levels in siRNA-Control group respect to sham, in accordance with bibliography. Nevertheless immunohistochemical results showed a modest induction of HIF1α protein in the infarct border zone.

Consistent with the mRNA expression data, a significant increase in Hif1α protein levels was observed in the MI siRNA-TRH group compared to MI siRNA-Control and Sham groups (Figure 5B).

To reinforce these findings, we measured the mRNA expression of VEGF and we observed as expected a significant increase in *VEGF* mRNA abundance in the MI siRNA control compared to sham-treated groups. In agreement, immunohistochemical results showed the same pattern. Strikingly, we observed a significant increase in *VEGF* mRNA abundance in MI siRNA-TRH treated group compared to MI siRNA control group (Figure 5C). In parallel a significant increase in VEGF protein levels was observed in the MI siRNA-TRH treated group compared to MI siRNA-Control and sham-treated groups (Figure 5D).

This result may account for the beneficial effects of the siRNA-TRH treatment in MI.

siRNA-TRH inhibition decrease oxidative stress following MI

Based on the role of oxidative stress in myocardial ischemia and infarction, we measured several antioxidant enzymes and oxidative stress markers.

As expected, there was a significant increase in the expression of Thioredoxin (Figure supplemental 3A), peroxiredoxin (supplemental 3B), nitrotyrosine (supplemental 3C), HSP70 (supplemental 3D) and HSP27 (supplemental 3E) in the peri-infarct area of the infarcted control rats compared to all groups ($p<0.01$) confirming the infarct injury induced in cardiac tissue. In contrast, silencing TRH in the MI group significantly reduced the protein immmunostaining of all these proteins in the peri-infarct area compared to MI siRNA-Control ($p<0.01$).

Collectively, these data demonstrated that, in addition to improving the LV function, siRNA-TRH inhibition decreases oxidative stress markers supporting an additional protective effect of the siRNA-TRH treatment.

siRNA-TRH inhibition reduces markers of hypoxia in an *in vitro* model emulating myocardial ischemia

To mimic the conditions of myocyte death *in vitro*, we use a model of hypoxia with increase expression of Hif1α(12). The cell line H9C2 was exposed to culture conditions that simulated ischemia.

We found the same pattern of a significant increased expression of TRH in the hypoxia group compared to the control group after 2 hours of hypoxic condition. The treatment with siRNA-TRH in the hypoxia group significantly reduced the *TRH* gene expression by two-fold, demonstrating the efficacy of the siRNA-TRH treatment. As expected, we found a significant increase in the expression of other hypoxia marker genes such as *GLUT4*, *VEGF,* and *GATA4,* as well as the apoptosis marker *Caspase 3* in the hypoxic, compared to normoxic conditions cells treated with siRNA-Control. There was a significant reduction in the expression of all these genes in the hypoxic siRNA-TRH group compared to hypoxic siRNA-control, similar to normoxic groups (Supplemental Figure 2).

These results demonstrate that hypoxic conditions *in vitro* increase the expression of *TRH* in cardiomyocytes. Moreover, TRH inhibition reduces the expression of markers of hypoxia in this model.

Discussion:

In this study we demonstrated that cardiac TRH inhibition improves LV systolic function and attenuates ventricular remodeling 1 week after MI. These novel findings support the idea that TRH inhibition may serve as a new therapeutic strategy to prevent the progression of heart failure.

Since the discovery of a TRH system in the heart, many authors have attempted to elucidate the function of local TRH in cardiac physiology (1, 13, 35), and both the mRNA and the protein were found in human heart tissue(4, 15, 28).

In animal models, it was described that its expression in cardiac tissue appears to be low under physiological conditions, as can be observed in sham animals (6, 11).

Our group has previously reported that adult SHRs show a LV TRH system hyperactivity only after the development of cardiac hypertrophy. Also, the long-term inhibition of the LV TRH system in young SHRs prevented cardiomyocyte enlargement, extracellular matrix expansion and fibrosis development. Moreover, the LVH index was lower and similar to their control Wistar Kyoto rats, at adult stages despite the persistent and severe hypertension still present in this model(29).

In parallel, Jin et al. showed that there is a sustained induction in the expression of LV *TRH* precursor mRNA in the scar and the peri-infarct myocardium up to 8 weeks after MI. Their model presents depressed cardiac function(17). Since then, no other studies have reported the role of cardiac TRH after infarction.

In this study, we confirm the induction of TRH in the infarcted heart and further demonstrated, for the first time in our knowledge, that *in vivo* inhibition of cardiac TRH by siRNA improved cardiac function and protected against cardiac remodeling after MI in rats. The beneficial effects included attenuation of hypertrophy, cardiac fibrosis, and LV enlargement.

One week after MI, animals with a TRH system blocked showed an improvement in cardiac function in comparison with rats infarcted with a native TRH system. Animals treated with siRNA-TRH presented higher EF and lower LVEDV and LVESV despite an unaltered infarct size. Moreover, infarcted control rats exhibited compensatory hypertrophy in the septum, and increased internal diameter of the left ventricle, which was prevented by TRH silencing. Then, specific TRH inhibition treatment normalized the

increase in the mass hypertrophy index one week after MI. Consistent with the fact that TRH inhibition effectively prevented the hypertrophy induced by MI *in vivo*, we found a decrease in the expression of all hypertrophy markers in the peri-infarct region, which is similar to a fetal gene expression pattern. These findings are also in agreement with our previous *in vitro* studies, where TRH overexpression in primary culture myocytes increased hypertrophic markers such as *BNP* and *βMHC*(30).

It is well known that collagen deposition and fibrosis play an essential role in cardiac remodeling after MI. Cardiac collagen remodeling occurs not only in the infarcted area, but also in remote areas from the infarct site(6). Notably, remodeling in the non-infarcted area is the primary contributor to ventricular remodeling(7). It has been shown that excessive accumulation of myocardial collagen might result in myocardial stiffness and severely impaired relaxation(9). In this study, we showed that TRH inhibition significantly attenuated the increase in the collagen deposition. Also, animals treated with the specific siRNA against TRH showed less fibrosis compared to animals treated with mismatch-siRNA. In agreement, mRNA levels of collagen type I and III, major components of the pericellular matrix, followed the same pattern. These data are in line with our previous results showing that TRH overexpression in cardiac fibroblast increased collagen synthesis *in vitro*(30) and that the profibrotic effect of the angiotensin II requires an intact cardiac TRH system to induce hypertrophy and fibrosis *in vivo* and *in vitro* (26).

Taken together, these data suggest that improvements in cardiac function by the specific LV TRH inhibition may be related to a reduction in i) cardiac hypertrophy, and ii) interstitial fibrosis in the peri-infarct region, without affecting perivascular fibrosis. Further mechanistic studies are required to elucidate the precise effect on profibrotic signaling cascades.

LV hypertrophy after MI seems to be an adaptative response to maintain the contractile function. However, in this study, we found a reduction in cardiac hypertrophy accompanied by a decrease in fibrosis, which, as a whole improves cardiac function in agreement with many other authors (33, 36).

Probably the most significant contribution of TRH inhibition in this scenario is the decrease in fibrosis, which causes less dilation and hypertrophy. Indeed the organ conserves a better ejection fraction with higher contractile force, which leads to a reduction in wall stress.

As speculated by Jankowsky et al.(16) and Jin et al.(17), in this context, LV TRH inhibition results in an improvement of cardiac function and may be a useful therapeutic approach.

Strikingly, pharmacological approaches or other gene therapies took more than three weeks to attenuate the ventricular remodeling reaching a similar reduction in collagen deposition as to one week TRH therapy inhibition(2, 34). Thereby we propose the TRH as an early player in the cardiac remodeling.

These results point out some advantages such as short treatment period with high local cardiac concentrations and fewer side effects (e.g. avoid hypotension) which could possibly be able to synergize the current treatments. Cultured cells under hypoxia could serve as a useful *in vitro* model for exploring infarction. We used the H9C2 cell line that exhibits electrophysiological and biochemical properties of cardiac tissue, without spontaneous contraction(14).

Hypoxic conditions induced a significant increase in hypoxic markers as well as TRH expression similar to those observed in the cardiac tissue of infarcted rats. In accordance, in this model, TRH inhibition effectively reduced the expression of hypoxic markers, *Glut4*, *Gata4, Vegf,* and *caspase* 3, indicating that they depend on TRH.

In the series of events after MI hypoxia-inducible factors may play a central role. It has been previously shown that higher amounts of HIF-1α in the heart improve cardiac performance, protect against the extension of infarction, and improve border zone survival in myocardial infarction(18). We observed that HIF-1α mRNA and its protein are significantly induced by TRH silencing.

HIF-1 controls several pathways critical for cellular response to hypoxia. One of them includes the transcriptional activation of angiogenic genes such as VEGF, and protection from oxidant stress (18). Antioxidant enzymes such as peroxiredoxins, thioredoxin, and Nitrotyrosine also contribute to cellular protection by reducing oxidized critical thiols in key enzymes/proteins and maintaining the suitable intracellular redox state. In addition to their peroxidase activity, they also act as molecular chaperones (22). We additionally measured the chaperones hsp27 y hsp70 which are known to acts as a biomarkers of heart failure (22) (20). The present study demonstrated that sirna-TRH inhibition exerted cardioprotective effects against myocardial injury also through the inhibition of oxidative stress.

Although further studies are necessary to define TRH mediators, we postulate that the HIF-1α induction mediated by TRH probably induce VEGF and might increase angiogenesis and attenuates the oxidative stress, therefore improving heart function. In conclusion, our findings show that the siRNA-TRH strategy was highly efficient and specific to downregulate the cardiac TRH system. We demonstrated that TRH inhibition induces an improvement in cardiac function and attenuates post-ischemic damage pointing it out as a relevant player in the post-MI remodeling. These novel findings may have important pathophysiological implications and suggest that TRH silencing may be a new promising therapeutic tool in the progression of heart failure.

Our study may have limitations. For example it is necessary to clarify the long term effects of TRH silencing on cardiac performance, and to elucidate which is the time

frame for the protective effect of the TRH silencing to occur after the MI trigger episode. Nonetheless, our studies strongly support the idea that cardiac TRH inhibition may serve as a putative gene therapy for maintaining cardiac function after MI.

Acknowledgements

The authors are grateful to Carlos J. Pirola, Ph.D, for revising this manuscript. We also thank Noelia Gonzales Mansilla, BVSc, for her technical assistance in animal care and Graciela Giardina for her technical assistance.

Funding

This work was supported by the National Council of Research and Technology (CONICET), Argentina [grant number PIP 1122012010049l] and National Agency of Research and Technology, ANPCyT Argentina [grant number BID-PICT N° 2016-0549].

Disclosures

The authors declare that they have no conflict of interest.

Author Contributions

Author contributions: Mariano L. Schuman, Ludmila S. Peres Diaz, Jorge E. Toblli and Maia Aisicovich performed experiments; Mariano L. Schuman, Jorge E. Toblli, and Silvia I. García analyzed data; Mariano L. Schuman , Maria S. Landa, Fernando Ingallina, and Silvia I. García interpreted results of experiments; Mariano L. Schuman, Maia Aisicovich, and Silvia I. García edited and revised manuscript; Silvia I. García conception and design of research; Mariano L. Schuman prepared figures; Mariano L. Schuman and Silvia I. García drafted manuscript; Mariano L. Schuman and Silvia I. García approved final version of manuscript.

References:

1. **Bačova Z**, **Baqi L**, **Beňačka O**, **Payer J**, **Križanová O**, **Zeman M**, **Smreková L**, **Zorad Š**, **Štrbák V**. Thyrotropin-releasing hormone in rat heart: Effect of swelling, angiotensin II and renin gene. *Acta Physiol* 187: 313–319, 2006. doi: 10.1111/j.1748-1716.2006.01545.x.

2. **Bernardo BC**, **Gao XM**, **Winbanks CE**, **Boey EJH**, **Tham YK**, **Kiriazis H**, **Gregorevic P**, **Obad S**, **Kauppinen S**, **Du XJ**, **Lin RCY**, **McMullen JR**. Therapeutic inhibition of the miR-34 family attenuates pathological cardiac remodeling and improves heart function. *Proc Natl Acad Sci U S A* 109: 17615–17620, 2012. doi: 10.1073/pnas.1206432109.

3. **Bès S**, **Ponsard B**, **El Asri M**, **Tissier C**, **Vandroux D**, **Rochette L**, **Athias P**. Assessment of the cytoprotective role of adenosine in an in vitro cellular model of myocardial ischemia. *Eur J Pharmacol* 452: 145–154, 2002. doi: 10.1016/S0014-2999(02)02295-1.

4. **Birket MJ**, **Raibaud S**, **Lettieri M**, **Adamson AD**, **Letang V**, **Cervello P**, **Redon N**, **Ret G**, **Viale S**, **Wang B**, **Biton B**, **Guillemot J-C**, **Mikol V**, **Leonard JP**, **Hanley NA**, **Orsini C**, **Itier J-M**. A Human Stem Cell Model of Fabry Disease Implicates LIMP-2 Accumulation in Cardiomyocyte Pathology. *Stem Cell Rep* 13: 380–393, 2019. doi: 10.1016/j.stemcr.2019.07.004.

5. **Carnell NE**, **Feng P**, **Kim UJ**, **Wilber JF**. Preprothyrotropin-releasing hormone mRNA and TRH are present in the rat heart. *Neuropeptides* 22: 209–212, 1992. doi: 10.1016/0143-4179(92)90047-Z.

6. **Cleutjens JPM**, **Verluyten MJA**, **Smits JFM**, **Daemen MJAP**. Collagen remodeling after myocardial infarction in the rat heart. *Am J Pathol* 147: 325–38., 1995.

7. **Czubryt MP**. Common threads in cardiac fibrosis, infarct scar formation, and wound healing. *Fibrogenesis Tissue Repair* 5: 19, 2012. doi: 10.1186/1755-1536-5-19.

8. **Del Rio-Garcia J**, **Smyth DG**. Distribution of pyroglutamylpeptide amides to thyrotrophin-releasing hormone in the central nervous system and periphery of the rat. *J Endocrinol* 127: 445–450, 1990. doi: 10.1677/joe.0.1270445.

9. **Doering CW**, **Jalil JE**, **Janicki JS**, **Pick R**, **Aghili S**, **Abrahams C**, **Weber KT**. Collagen network remodelling and diastolic stiffness of the rat left ventricle with pressure overload hypertrophy. *Cardiovasc Res* 22: 686–695, 1988. doi: 10.1093/cvr/22.10.686.

10. **Dokainish H**, **Nguyen JS**, **Bobek J**, **Goswami R**, **Lakkis NM**. Assessment of the American Society of Echocardiography-European Association of Echocardiography guidelines for diastolic function in patients with depressed ejection fraction: An

echocardiographic and invasive haemodynamic study. *Eur J Echocardiogr* 12: 857–864, 2011. doi: 10.1093/ejechocard/jer157.

11. **García SI**, **Alvarez AL**, **Porto PI**, **Garfunkel VM**, **Finkielman S**, **Pirola CJ**. Antisense inhibition of thyrotropin-releasing hormone reduces arterial blood pressure in spontaneously hypertensive rats. *Hypertension* 37: 365–370, 2001. doi: 10.1161/01.hyp.37.2.365.

12. **Gui L**, **Liu B**, **Lv G**. Hypoxia induces autophagy in cardiomyocytes via a hypoxia-inducible factor 1-dependent mechanism. *Exp Ther Med* 11: 2233–2239, 2016. doi: 10.3892/etm.2016.3190.

13. **Hasegawa J**, **Hirai S**, **Kotake H**, **Hisatome I**, **Mashiba H**. Inotropic effect of thyrotropin-releasing hormone on the guinea pig myocardium. *Endocrinology* 12: 2805–2811, 1988. doi: 10.1210/endo-123-6-2805.

14. **Hescheler J**, **Meyer R**, **Plant S**, **Krautwurst D**, **Rosenthal W**, **Schultz G**. Morphological, biochemical, and electrophysiological characterization of a clonal cell (H9c2) line from rat heart. *Circ Res* 69: 1476–1486, 1991. doi: 10.1161/01.RES.69.6.1476.

15. **Iborra-Egea O**, **Santiago-Vacas E**, **Yurista SR**, **Lupón J**, **Packer M**, **Heymans S**, **Zannad F**, **Butler J**, **Pascual-Figal D**, **Lax A**, **Núñez J**, **de Boer RA**, **Bayés-Genís A**. Unraveling the Molecular Mechanism of Action of Empagliflozin in Heart Failure With Reduced Ejection Fraction With or Without Diabetes. *JACC Basic Transl Sci* 4: 831–840, 2019. doi: 10.1016/j.jacbts.2019.07.010.

16. **Jankowski M**. Cardiac delivery of interference RNA for thyrotropin-releasing hormone inhibits hypertrophy in spontaneously hypertensive rat. *Hypertension* 57: 26–28, 2011. doi: 10.1161/HYPERTENSIONAHA.110.163477.

17. **Jin H**, **Fedorowicz G**, **Yang R**, **Ogasawara A**, **Peale F**, **Pham T**, **Paoni NF**. Thyrotropin-Releasing Hormone Is Induced in the Left Ventricle of Rats with Heart Failure and Can Provide Inotropic Support to the Failing Heart. *Circulation* 109: 2240–2245, 2004. doi: 10.1161/01.CIR.0000127951.13380.B4.

18. **Kido M**, **Du L**, **Sullivan CC**, **Li X**, **Deutsch R**, **Jamieson SW**, **Thistlethwaite PA**. Hypoxia-inducible factor 1-alpha reduces infarction and attenuates progression of cardiac dysfunction after myocardial infarction in the mouse. *J Am Coll Cardiol* 46: 2116–2124, 2005. doi: 10.1016/j.jacc.2005.08.045.

19. **Landa MS**, **García SI**, **Schuman ML**, **Peres Diaz LS**, **Aisicovich M**, **Pirola CJ**. Cardiovascular and body weight regulation changes in transgenic mice overexpressing thyrotropin-releasing hormone (TRH). J Physiol Biochem. doi:10.1007/s13105-020-00765-x

20. **Latchman D**. Heat shock proteins and cardiac protection. *Cardiovasc Res* 51: 637–646, 2001. doi: 10.1016/S0008-6363(01)00354-6.

21. **Lee SH**, **Wolf PL**, **Escudero R**, **Deutsch R**, **Jamieson SW**, **Thistlethwaite PA**. Early expression of angiogenesis factors in acute myocardial ischemia and

infarction. *N Engl J Med* 342: 626–633, 2000. doi: 10.1056/NEJM200003023420904.

22. **Li Z**, **Song Y**, **Xing R**, **Yu H**, **Zhang Y**, **Li Z**, **Gao W**. Heat Shock Protein 70 Acts as a Potential Biomarker for Early Diagnosis of Heart Failure. *PLoS ONE* 8: e67964, 2013. doi: 10.1371/journal.pone.0067964.

23. **Mattila J**, **Bunag RD**. Pressor and sympathetic responses to dorsal raphe nucleus infusions of TRH in rats. *Am J Physiol - Regul Integr Comp Physiol* 258: R1464–R1471, 1990. doi: 10.1152/ajpregu.1990.258.6.r1464.

24. **Morley JE**. Extrahypothalamic Thyrotropin Releasing Hormone (TRH) - Its distribution and its functions. *Life Sci* 25: 1539–1550, 1979. doi: 10.1016/0024-3205(79)90435-1.

25. **Nillni EA**, **Sevarino KA**. The biology of pro-thyrotropin-releasing hormone-derived peptides. *Endocr Rev* 20: 599–648, 1999. doi: 10.1210/edrv.20.5.0379.

26. **Peres Diaz LS**, **Schuman ML**, **Aisicovich M**, **Toblli JE**, **Pirola CJ**, **Landa MS**, **García SI**. Angiotensin II requires an intact cardiac thyrotropin-releasing hormone (TRH) system to induce cardiac hypertrophy in mouse. *J Mol Cell Cardiol* 124: P1-11, 2018. doi: 10.1016/j.yjmcc.2018.09.009.

27. **Peres Diaz LS**, **Schuman ML**, **Aisicovich M**, **Toblli JE**, **Pirola CJ**, **Landa MS**, **García SI**. Short-term doxorubicin cardiotoxic effects: involvement of cardiac Thyrotropin Releasing Hormone system. *Life Sci* 261: 118346, 2020. doi: 10.1016/j.lfs.2020.118346.

28. **Pervolaraki E**, **Dachtler J**, **Anderson RA**, **Holden AV**. The developmental transcriptome of the human heart. *Sci Rep* 8: 15362, 2018. doi: 10.1038/s41598-018-33837-6.

29. **Schuman ML**, **Landa MS**, **Toblli JE**, **Peres Diaz LS**, **Alvarez AL**, **Finkielman S**, **Paz L**, **Cao G**, **Pirola CJ**, **García SI**. Cardiac thyrotropin-releasing hormone mediates left ventricular hypertrophy in spontaneously hypertensive rats. *Hypertension* 57: 103–109, 2011. doi: 10.1161/HYPERTENSIONAHA.110.161265.

30. **Schuman ML**, **Peres Diaz LS**, **Landa MS**, **Toblli JE**, **Cao G**, **Alvarez AL**, **Finkielman S**, **Pirola CJ**, **García SI**. Thyrotropin-releasing hormone overexpression induces structural changes of the left ventricle in the normal rat heart. *Am J Physiol - Heart Circ Physiol* 307: H1667–H1674, 2014. doi: 10.1152/ajpheart.00494.2014.

31. **Semenza GL**. Hypoxia-Inducible Factor 1 and Cardiovascular Disease. *Annu Rev Physiol* 76: 39–56, 2014. doi: 10.1146/annurev-physiol-021113-170322.

32. **Socci R**, **Kolbeck RC**, **Mészáros LG**. Positive inotropic effect of thyrotropin-releasing hormone on isolated rat hearts. *Gen Physiol Biophys* 4: 309–16, 1996.

33. **Von Lueder TG**, **Wang BH**, **Kompa AR**, **Huang L**, **Webb R**, **Jordaan P**, **Atar D**, **Krum H**. Angiotensin receptor neprilysin inhibitor LCZ696 attenuates cardiac remodeling and dysfunction after myocardial infarction by reducing cardiac fibrosis

and hypertrophy. *Circ Heart Fail* 8: 71–78, 2015. doi: 10.1161/CIRCHEARTFAILURE.114.001785.

34. **Wei Q**, **Liu H**, **Liu M**, **Yang C**, **Yang J**, **Liu Z**, **Yang P**. Ramipril attenuates left ventricular remodeling by regulating the expression of activin A-follistatin in a rat model of heart failure. *Sci Rep* 6, 2016. doi: 10.1038/srep33677.

35. **Wilber JF**, **Xu AH**. The thyrotropin-releasing hormone gene 1998: Cloning, characterization, and transcriptional regulation in the central nervous system, heart, and testis. *Thyroid* 8: 897–901, 1998. doi: 10.1089/thy.1998.8.897.

36. **Yamazaki T**, **Izumi Y**, **Nakamura Y**, **Yamashita N**, **Fujiki H**, **Osada-Oka M**, **Shiota M**, **Hanatani A**, **Shimada K**, **Iwao H**, **Yoshiyama M**. Tolvaptan improves left ventricular dysfunction after myocardial infarction in rats. *Circ Heart Fail* 5: 794–802, 2012. doi: 10.1161/CIRCHEARTFAILURE.112.968750.

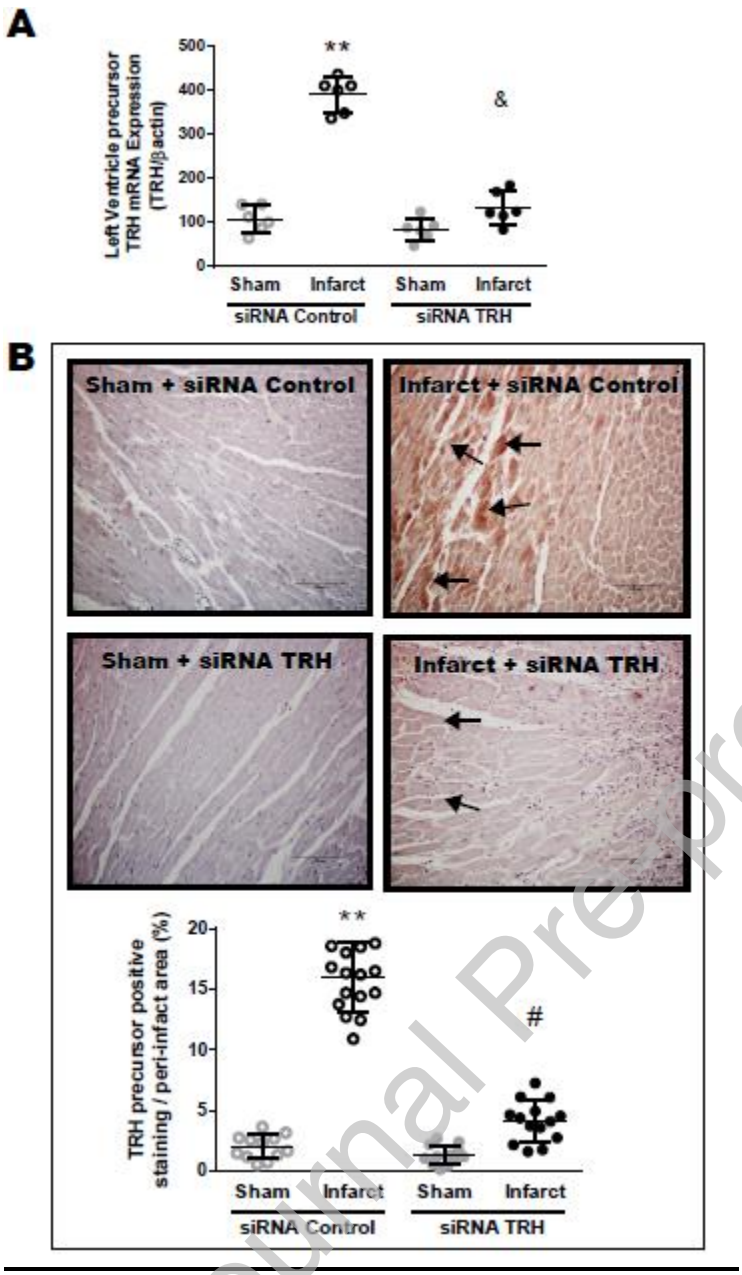

Figure 1. Effects of MI on TRH expression: (A) Expression levels of mRNA *preproTRH* normalized by *β-actin* expression in the infarct border zone after MI by quantitative RT-PCR. (n=6 per group), ***p*<0.01 versus all groups. &*p*<0.05 versus Sham + siRNA-Control and Sham + siRNA-TRH. Results are expressed as percentage of control group. (B) Representative TRH immunohistochemistry of the peri-infarct region using an anti-TRH precursor antibody (n=6 rats per group). (200× magnification) Scale bar represents 100µm. ***p*<0.01 versus all groups, #*p*<0.01 versus Sham+ siRNA-Control and Sham+ siRNA-TRH. Significant differences in positive immunostaining (arrows)

were observed between infarcted animals injected with siRNA-TRH and siRNA-Control groups

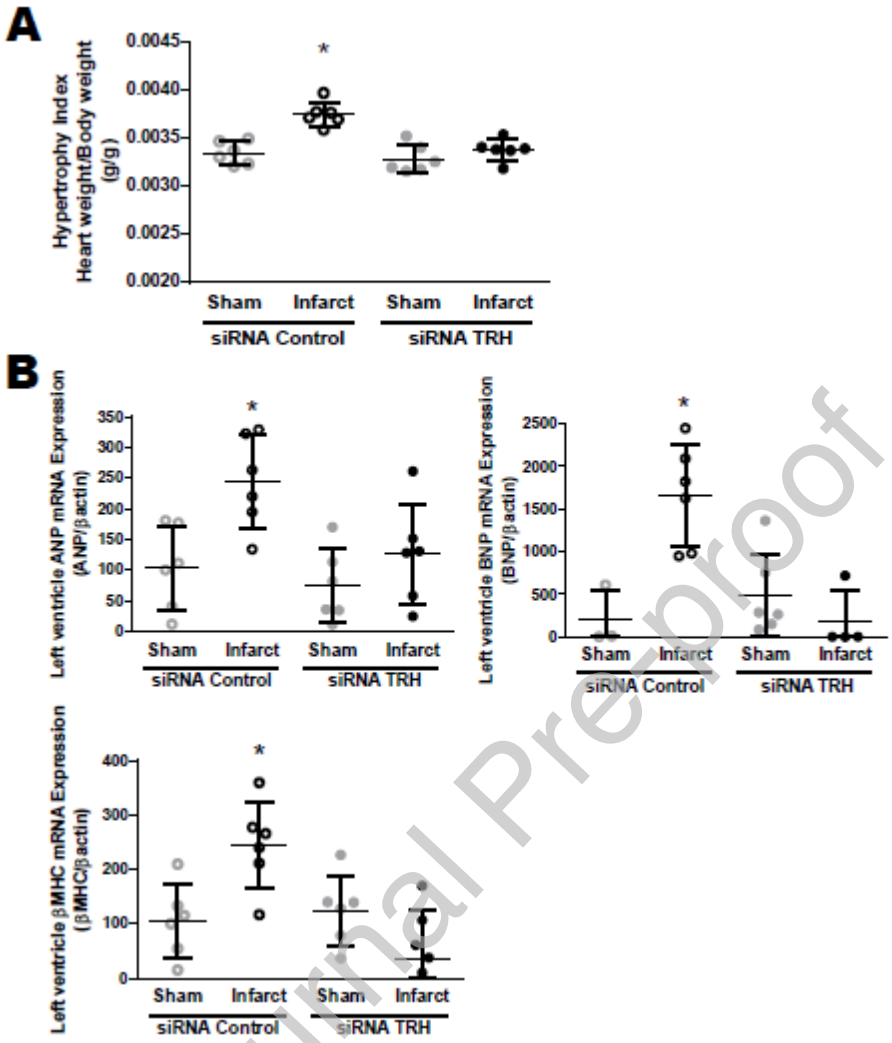

Figure 2. siRNA-TRH inhibition reduces hypertrophy in response to MI. (A) Hypertrophy index Heart weight/Body weight ratio 1 week after MI remodeling. (n=6 per group) * $p<0.05$ versus all groups (B) Expression levels of mRNAs associated with hypertrophy by quantitative RT-PCR normalized by *β-actin* expression in the LV infarct border zone, *$p<0.05$ versus all groups. (n=6 rats per group). Results are expressed as percentage of control group. *ANP*, Atrial *natriuretic* peptide. *BNP*, B-type natriuretic peptide . *βMHC*, beta *myosin heavy chain.*

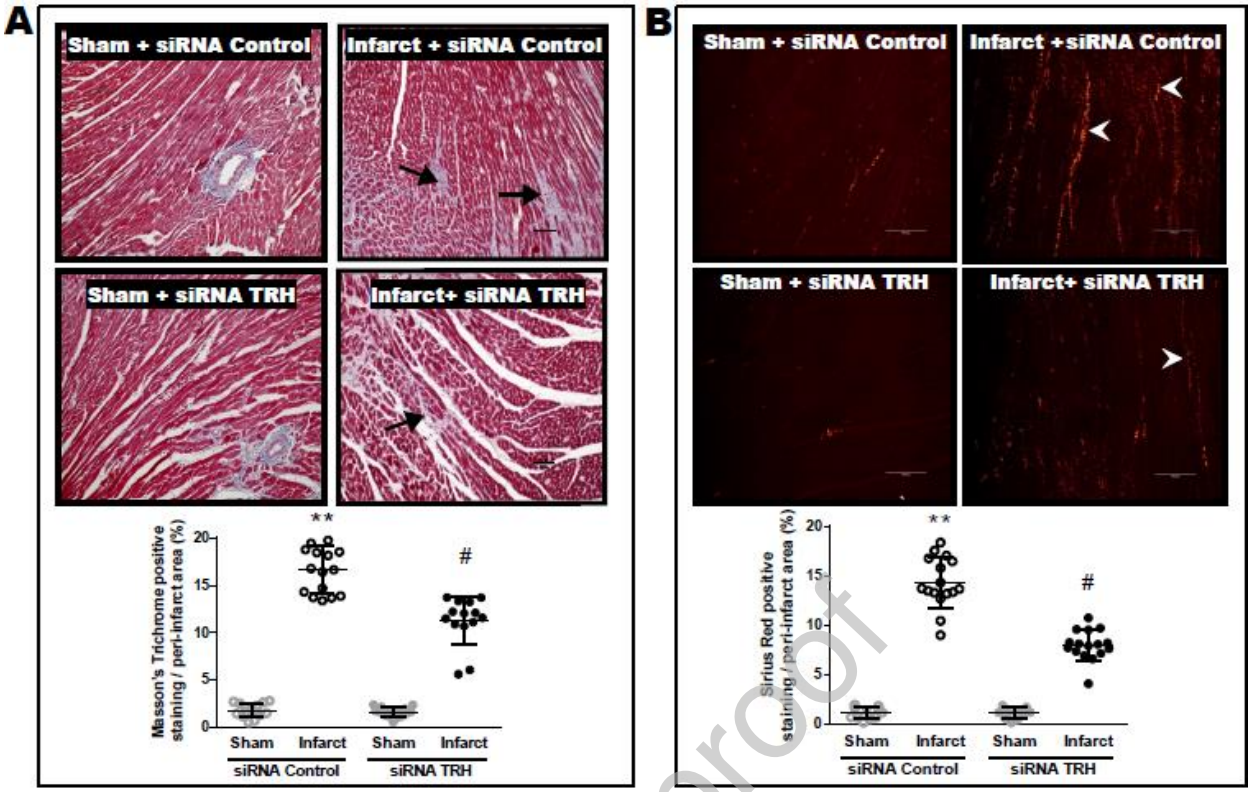

Figure 3. siRNA-TRH inhibition reduces peri-infarct myocardial fibrosis following MI. (A) Representative images of Masson's trichrome-stained and (B) Sirius red polarized light micrographs staining heart sections in the infarct border zone (n=6 per group) 1 week after MI remodeling (200X magnification). Scale bar represents 100µm. ***p*<0.01 versus all groups. #*p*<0.01 versus Sham + siRNA-Control and Sham + siRNA-TRH. Significant differences in ECM expansion (arrows) were observed between infarcted animals injected with siRNA-TRH and siRNA-Control groups

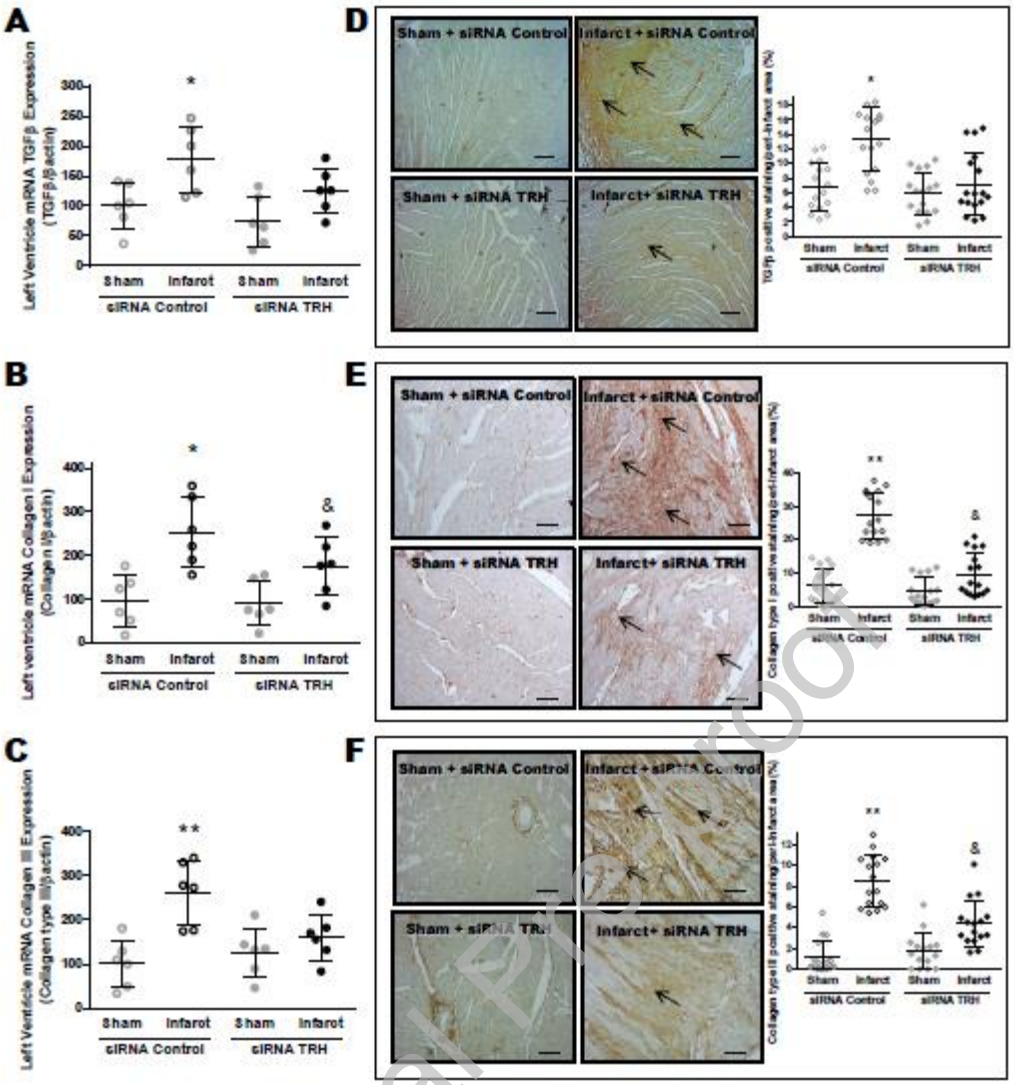

Figure 4. siRNA-TRH inhibition reduces peri-infarct myocardial fibrosis following MI. Expression levels of mRNAs by quantitative RT-PCR normalized by *β-actin* expression in the LV infarct border zone of (A) *TGFβ*, (B) *collagen type I* and (C) *collagen type III*. (n=6 per group). Results are expressed as percentage of control group.

Representative Immunohistochemical staining with (D) anti-TGFβ, (E) anti-Collagen type I and (F) anti-Collagen type III monoclonal antibody hearts (n=6 for each group) 1 week after coronary ligation in the LV peri-infarct region (200X magnification). Scale bar represents 100µm. Quantitative analysis is shown on the right of each image. ***p*<0.01 versus all groups. **p*<0.05 versus all groups. *&p*<0.05 versus Sham + siRNA-Control and Sham + siRNA-TRH. TGFβ, Transforming growth factor -β1. Significant differences

in positive immunostaining (arrows) were observed between infarcted animals injected with siRNA-TRH and siRNA-Control groups

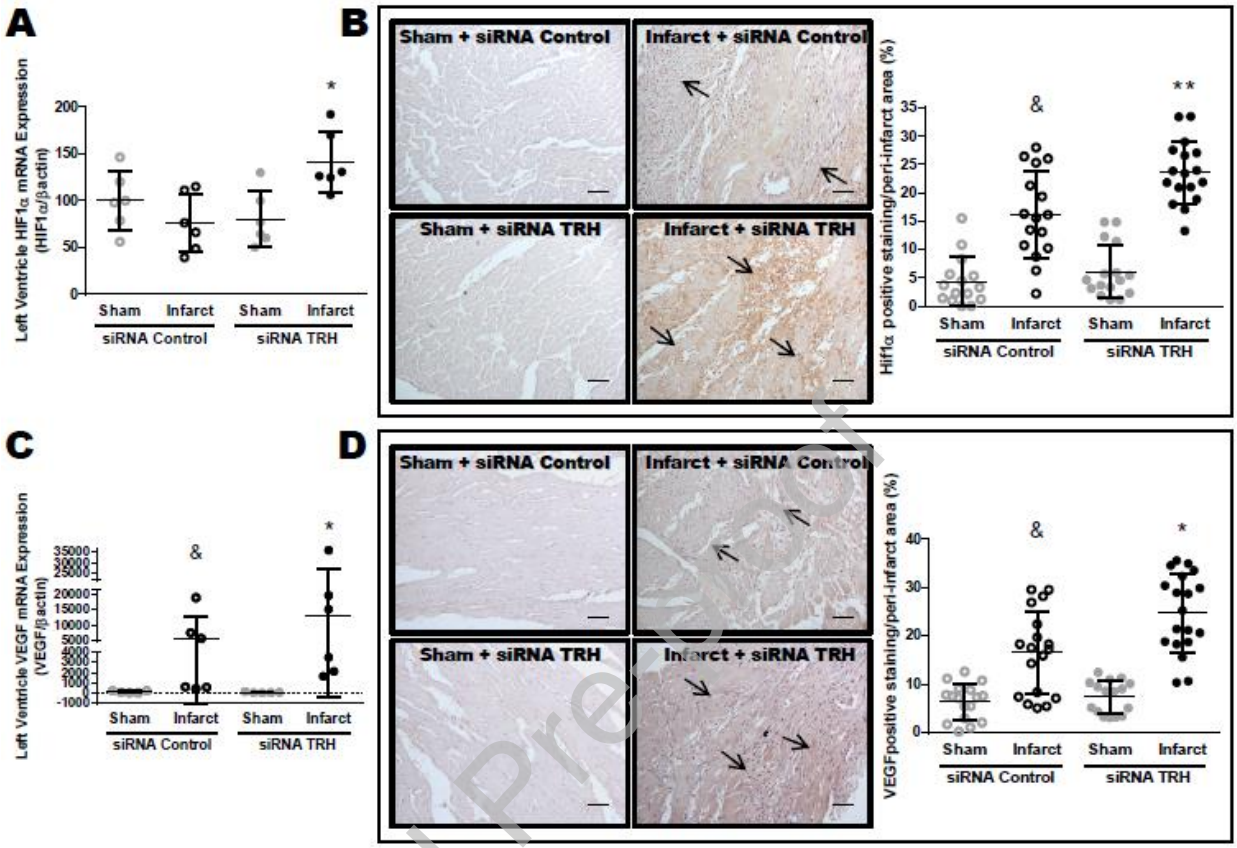

Figure 5. siRNA-TRH inhibition increase Hif1α and VEGF following MI. (A) Expression levels of *Hif1α* mRNA normalized by *β-actin* expression in the infarct border zone after MI by quantitative RT-PCR. (n=6 per group), *p<0.05 vs. all groups. Results are expressed as percentage of control group. (B) Representative Hif1α immunohistochemistry of the LV peri-infarct region (n=6 per group). (C) Expression levels of *VEGF* mRNA normalized by *β-actin* expression in the infarct border zone after MI by quantitative RT-PCR. Results are expressed as percentage of control group (n=6 per group). (D) Representative VEGF immunohistochemistry of the LV peri-infarct region (n=6 per group) (200X magnification)**.** Scale bar represents 100μm. Quantitative analysis is shown on the right of the image. **p<0.01 versus all groups, &p<0.05 versus Sham + siRNA-Control and Sham + siRNA-TRH. Significant differences in positive

inmunostaining (arrows) were observed between infarcted animals injected with siRNA-TRH and siRNA-Control groups.

Tables

TABLE 1 Echocardiographic parameters six days after the induction of MI.

	Sham + siRNA-Control (n=6)	Infarct + siRNA-Control (n=6)	Sham + siRNA-TRH (n=6)	Infarct + siRNA-TRH (n=6)
IVSd (cm)	0.156 ± 0.007	0.176 ± 0.009 *	0.151 ± 0.009	0.152 ± 0.008 #
IVSs (cm)	0.269 ± 0.015	0.279 ± 0.011	0.264 ± 0.019	0.268 ± 0.014
LVIDd (cm)	0.679 ± 0.025	0.902 ± 0.027 **	0.732 ± 0.032	0.827 ± 0.029 ##
LVIDs (cm)	0.387 ± 0.024	0.689 ± 0.036 **	0.405 ± 0.032	0.556 ± 0.027 ##
LVPWd (cm)	0.226 ± 0.011	0.186 ± 0.012	0.205 ± 0.015	0.179 ± 0.012
LVPWs (cm)	0.278 ± 0.020	0.260 ± 0.015	0.262 ± 0.0238	0.271 ± 0.018
LVEDV (ml)	0.767 ± 0.115	1.339 ± 0.102 **	0.827 ± 0.121	1.049 ± 0.102 #
LVESV (ml)	0.102 ± 0.051	0.515 ± 0.037 **	0.181 ± 0.051	0.282 ± 0.043 ##
SF (%)	51.59 ± 2.21	30.34 ± 2.55**	45.43 ± 3.53	37.31 ± 2.55
EF (%)	86.30 ± 2.47	65.69 ± 2.85 **	82.96 ± 3.35	71.89 ± 2.80 #
SV (ml)	0.672 ± 0.063	0.719 ± 0.069	0.766 ± 0.069	0.837 ± 0.063
HR (Beats/min)	193 ± 14	238 ± 11 *	196 ± 17	198 ± 12 #

Data are presented as mean value ± SEM.

Abbreviations: IVSd, Interventricular Septum thickness in diastole; IVSs, Interventricular Septum thickness in systole; LVIDd, left ventricular internal diameter in diastole; LVIDs, left ventricular internal diameter in systole; LVPWd, Left ventricular posterior wall thickness in diastole; LVPWs, Left ventricular posterior wall thickness in systole; LVEDV, Left ventricular end diastolic volume; LVESV, Left ventricular end systolic volume; SF, shortening fraction; EF, Ejection fraction; SV, Stroke volume; HR, Heart rate.

* $p<0.05$ and ** $p<0.01$ vs. Sham + siRNA-Control and Sham+ siRNA-TRH, # $p<0.05$ and ##$p<0.01$ vs. Infarct + siRNA-Control.